# Gas Phase Infrared Spectroscopy of Selectively Prepared Ions

J. Lemaire,[1] P. Boissel,[1] M. Heninger,[1] G. Mauclaire,[1] G. Bellec,[1] H. Mestdagh,[1] A. Simon,[1] S. Le Caer,[1] J. M. Ortega,[2]
F. Glotin,[2] and P. Maitre[1,*]

[1]*Laboratoire de Chimie Physique (UMR 8000–CNRS), Batiment 350, Université Paris XI, 91405 Orsay Cedex, France*
[2]*CLIO-LURE, Batiment 209D, Université Paris XI, 91405 Orsay Cedex, France*

(Received 19 June 2002; published 18 December 2002)

The first example of direct structural characterization of polyaromatic ions by coupling a Fourier transform ion cyclotron resonance mass spectrometer with an infrared free-electron laser is presented. Measurement of the IR spectra of selectively prepared ionic reactive intermediates is allowed by the association of the high peak power and wide tunability of the laser with the flexibility of the spectrometer, where several mass selection and ion reaction steps can be combined, as demonstrated in the case of iron cation complexes of hydrocarbons. The present experimental setup opens the way to understanding chemical reaction paths.

DOI: 10.1103/PhysRevLett.89.273002 PACS numbers: 33.20.–t, 33.80.–b, 36.20.Ng, 82.50.Bc

Gas phase study of mass-selected metal containing ions has been shown to unravel the intrinsic physical and chemical properties of organometallic building blocks [1]. With this respect, Fourier transform ion cyclotron resonance mass spectrometry (FT-ICR-MS) is an interesting technique for offering complex schemes for ion preparation which may combine mass selection, ion-molecule reactions, and fragmentation induced by collision with a buffer gas or photons [2]. Thermochemical information on such selectively prepared ions can be determined [3]. Some structural information can be derived from their reactivity of fragmentation behavior, and also by comparison with theory, but these approaches are rather indirect.

Therefore, the development of a direct structural characterization of mass-selected ions in an FT-ICR-MS would be very interesting. In this respect, infrared spectroscopy is the ideal approach, but obtaining the spectrum of isolated gas phase ions is a challenging problem. High resolution infrared spectroscopy of small molecular ions had been realized [4,5], where ions were produced by an electric discharge in a plasma. This approach provides ion column density in the $10^{13}$–$10^{16}$ $\mathrm{cm}^{-2}$ range, thus allowing for the detection of laser beam absorption. Under FT-ICR-MS conditions, however, ions are confined within a spot of the order of a $\mathrm{mm}^3$ at a density typically of $10^8$ $\mathrm{cm}^{-3}$, thus leading to an ion column density of $10^7$ $\mathrm{cm}^{-2}$. This, together with the weakness of the infrared transitions involved, prevents the use of absorption spectroscopy. Alternatively, photon absorption can be probed by monitoring the fragmentation of the ion induced by the subsequent raise in internal energy. As the energy required for dissociation is greater than that of the infrared photon, the messenger technique can be used. In this technique one probes the loss of a weakly bound atom [6] or molecule [7] attached to the ion of interest. Higher internal energies can be reached using intense laser sources allowing for infrared multiphoton dissociation (IRMPD).

IRMPD spectroscopy requires a high peak power, relatively small bandwidth, and easy tunability of the infrared laser source. These characteristics can be found at the CLIO infrared free-electron laser (FEL) facility at Orsay [8]. The FEL CLIO is based on a 10 to 50 MeV electron accelerator and has a very large wavelength range in the infrared (from 3 to 90 $\mu$m). Continuous tunability is obtained over a spectral range $\Delta\lambda/\lambda \approx 2.5$. The FEL relative bandwidth is typically 0.3% when the optical cavity is tuned in order to minimize it (at the expense of the peak power). The FEL temporal structure consists of macropulses about 8 $\mu$s long, at a repetition rate of 25 Hz, containing typically 500 micropulses a few picoseconds long each, separated by 16 ns. The typical energy content of a macropulse is 25 mJ with a peak power of 20 MW in each micropulse. The pulse-to-pulse reproducibility is a few percent and is continuously monitored with a detector. A fast electromechanical shutter synchronized with the laser allows the selection of a given number of macropulses, down to a single one. The beam is focused by a spherical mirror of 1 m focal length through a ZnSe entrance window.

The IRMPD of ions has recently been successfully applied to polycyclic aromatic hydrocarbon (PAH) cations at the FEL facility FELIX [9–11] and to organometallic complexes [12]. Nevertheless, due to limitations in mass resolution and ion preparation techniques, these studies were restricted to primary ions, and hydrogen loss dissociation channels could not be clearly resolved.

FT-ICR-MS gives access to a much broader range of ions, through ion-molecule reaction with a pulsed neutral gas and subsequent mass selection of a given product which can then be stored in a collision free environment up to several minutes. Ions are confined within a spot of 1 $\mathrm{mm}^3$, allowing for a good overlap with the laser beam.

Finally, the most interesting feature of the FT-ICR-MS is its high-mass resolution, 30 000 in the present case, essential for probing hydrogen loss under IRMPD. Evidence for IRMPD of ions trapped in an FT-ICR-MS cell has been shown using $CO_2$ laser [13]. Nevertheless, the coupling of an infrared FEL to classical FT-ICR-MS devices, due to their size and weight, has never been realized to provide the whole infrared spectrum of a molecular ion. The present experiment has been made possible by the recent construction in our laboratory of MICRA (mobile ICR analyzer), a compact FT-ICR spectrometer using a permanent magnet. The open-ended structure of the ICR cell provides a good optical access to its center. A detailed description of this device will be given elsewhere; here we present only a summary of its characteristics: magnetic field 1.25 T, mass range 10–1000 amu, mass resolution 30 000 at mass 131. Primary ions are produced by electron impact on neutral gas. The whole set of ion manipulation methods provided by FT-ICR-MS (mass selection, ion-molecule reactions, collision induced dissociation, etc.) can then be used to produce the desired type of ion. Gases are introduced using a leak valve followed by a threeway pulsed valve. The reproducibility of the gas pulse characteristics leads to a very good shot to shot stability of the ion intensities, which is essential to ensure the reproducibility of the mass analysis and hence a good signal to noise ratio in the final infrared spectrum.

Preliminary studies have been performed on $Fe(CO)_5{}^+$ ions to characterize the multiphoton fragmentation process. The detailed results will be analyzed in a separate paper; here we present only the points that are relevant for the spectroscopic studies. When the wavelength is set at the center of the absorption line, a 12 macropulses long irradiation at an average power of 500 mW leads to a nearly complete disappearance of the parent ion, and the series of $Fe(CO)_n{}^+$ with $n = 1$–4 is produced by a cascade of photodissociation. Figure 1 gives the normalized amount of the parent ion $P$ (ratio of the parent ion peak to the sum of all the peaks), in a logarithmic scale, as a function of the number of macropulses (1 to 12). Using a set of attenuators, the data were recorded for four different average laser powers. Concerning the use of IRMPD as a spectroscopic tool, two main conclusions can be drawn: (i) For the four laser powers used [Fig. 1(a)], the logarithmic representation shows that the parent ion peak $P$ exhibits an exponential decay with respect to the number $n$ of macropulses. This strongly suggests that the 40 ms separating two macropulses is sufficient for the nonfragmented remaining parent ions to relax before the next macropulse. That is, one can consider that each macropulse acts independently. (ii) Then, one can define an IRMPD pulse efficiency $E$ by the slope of the linear fits of Fig. 1(a). As can be seen in Fig. 1(b), at low laser power, there is a linear behavior of $E$ as a function of the average laser power, which is consistent with the theoretical model of Black *et al.* [14]. At higher laser power, saturation effects are observed. In the experiments of Dietrich *et al.* on dissociation of $Au_n$-methanol$^+$ cations [15] and of Oomens *et al.* [11], a nonlinear dependence is observed at low energies, due to the multiphoton character of the process. Data in Fig. 1 would suggest that this energy range is not probed here and that, provided $E$ is lower than 0.1 to avoid saturation, the pulse efficiency $E$ can be taken as a measure of the absorption cross section.

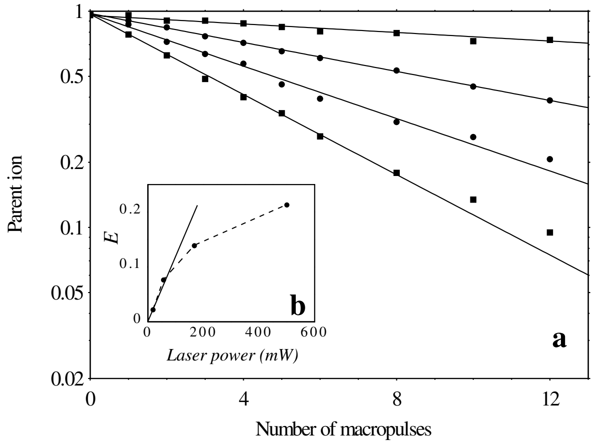

FIG. 1. Photodissociation of $FeCO_5{}^+$: Remaining parent ion as a function of the number of macropulses for four laser average powers: 18, 56, 170, and 500 mW from top to bottom (a) and fragmentation efficiency $E$ (see text) versus laser power (b)

Our main objective using IRMPD is to directly probe the structure of reactive intermediates. These data would complement those obtained both experimentally and theoretically in our laboratory on the reactivity of cationic metal complexes of CO [16] and hydrocarbons [17]. In this perspective, infrared spectroscopy of $Fe^+$ complexes of hydrocarbons has been undertaken and theoretical spectra derived from *ab initio* calculations are compared to the experimental results. $FeC_4H_8{}^+$ ions have been generated by ligand displacement of CO from $Fe(CO)^+$ by but-1-ene. $Fe(CO)^+$ is mass selected from the ions obtained by electron impact ionization on neutral $Fe(CO)_5$. After reaction with but-1-ene $FeC_4H_8{}^+$ ions ($m/z = 112$) are selected, then allowed to relax during 1 s before a 25 macropulse long irradiation. Two photofragments were observed: $Fe^+$ ($m/z = 56$) and $FeC_4H_6{}^+$ ($m/z = 110$). The good mass resolution provided by FT-ICR-MS is important here to properly monitor the relative intensity of $FeC_4H_6{}^+$, differing from the parent ion by only two mass units. Figure 2(a) displays the evolution of the mass peaks corresponding to the parent and the two fragments as a function of the wavelength. As can be seen, photofragmentation into $FeC_4H_6{}^+$ corresponding to the loss of $H_2$ is the dominant channel. The photofragment $Fe^+$ is produced only when the $FeC_4H_8{}^+$ parent ions are irradiated with low energy photons

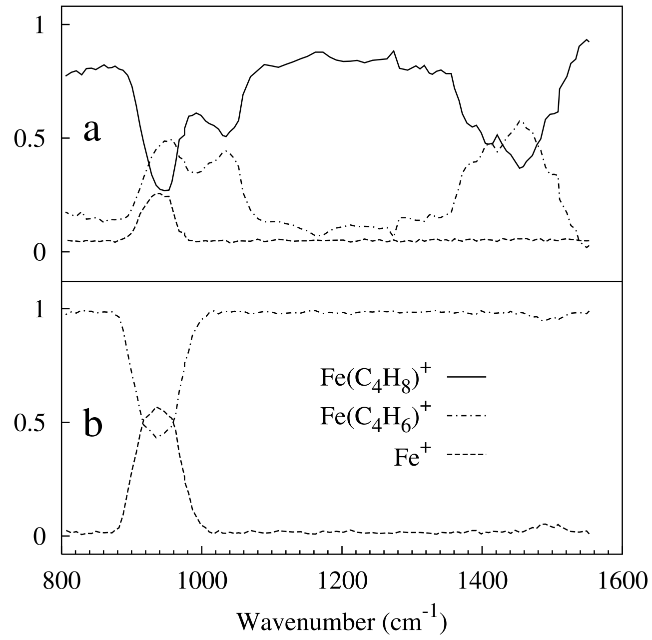

FIG. 2. Evolution of the parent and photofragment ions as a function of the wavelength using an average laser power of ca. 500 mW. Parent ions are $FeC_4H_8{}^+$ (a) and $FeC_4H_6{}^+$ (b).

ranging from 900 through 1000 $cm^{-1}$, with a maximum efficiency at 942 $cm^{-1}$.

Direct loss of $C_4H_8$ is much higher in energy than $H_2$ loss. The multiphoton dissociation process that is known to provide a slow heating of the ions is expected to lead preferentially to the lowest exit channels. Appearance of the $Fe^+$ cation is then probably due to a sequential process. This has been checked by monitoring the IRMPD of $FeC_4H_6{}^+$, which has been directly prepared through dehydrogenation of but-1-ene by mass-selected $Fe^+$. The evolution of the intensity of $Fe^+$ as a function of the photon wavelength is essentially the same when it is derived from the photofragmentation of $FeC_4H_8{}^+$ [Fig. 2(a)] or $FeC_4H_6{}^+$ [Fig. 2(b)]. This confirms that the photofragmentation of $FeC_4H_8{}^+$ is a sequential process: IRMPD of this ion produces $FeC_4H_6{}^+$, which photofragments into $Fe^+$ only when $FeC_4H_6{}^+$ can resonantly absorb photons, i.e., around 942 $cm^{-1}$.

The present results can be compared to that obtained by Surya and co-workers [18] using IRMPD with a $CO_2$ laser, collision induced dissociation (CID), and sustained off resonance irradiation (SORI), this latter method being also known for providing slow heating of the ions [3]. With SORI and IRMPD, only the loss of $H_2$ was observed. Loss of $H_2$ was also the only fragmentation pathway observed in low energy CID, and $Fe^+$ fragments were obtained only at high collision energy [18]. Interestingly, whereas the photon wave number of the $CO_2$ laser (944 $cm^{-1}$) is essentially the same as the one giving the maximum rate of $Fe^+$ in the present experiment, Surya and co-workers observed only the $H_2$ loss. This suggests that the lower peak power and smaller bandwidth of the continuous $CO_2$ laser prevent further absorption of photons by the $FeC_4H_6{}^+$ fragment.

Figure 3 gives the final IRMPD spectrum of the $FeC_4H_8{}^+$ ion. The vertical scale is the fragmentation efficiency, which, as explained above, should be proportional to the absorption cross section. Based on predicted harmonic vibrational transitions, photon energies ranging from 800 through 1600 $cm^{-1}$ have been scanned, using increments of 10 $cm^{-1}$. This whole spectrum has been recorded using a single electron energy (50 MeV).

The calculated harmonic vibrational bands of the Fe(but-1-ene)$^+$ complex are shown as a bar spectrum in Fig. 3. The electronic structure calculations used a hybrid density functional method (so-called B3LYP as implemented in GAUSSIAN98 [19]. Kohn-Sham orbitals were expanded in the same contracted basis set as the one employed to characterize the vibrational modes of $V^+(\text{benzene})_{1-2}$ [12]. The density functional theory, and particularly the hybrid B3LYP functional, has been shown to be very efficient for the prediction of harmonic frequencies. Fe(but-1-ene)$^+$ was found in a quartet ground state, as found by Sodupe *et al.* [20] for $Fe(C_2H_4)^+$. The elongation of the C=C bond (1.40 instead of 1.34 in the free ligand) is a typical signature of the strong metal to $\pi^*_{CC}$ donation.

The laser bandwidth together with the dynamics of the multiphoton excitation are responsible for the broadening of the bands [11]. The high density of electronic states of unsaturated organometallic species might also contribute to the broadening. In order to account for these effects

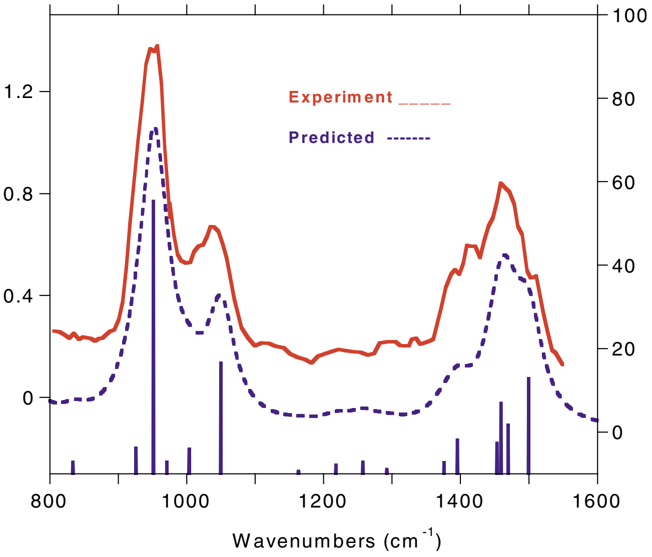

FIG. 3 (color online). IRMPD spectrum of $FeC_4H_8{}^+$ compared to the calculated bar spectrum and to a spectrum convoluted with a Lorentzian profile (dotted line). The left hand scale represents the IRMPD efficiency and the right one the calculated infrared intensities (km mol$^{-1}$

and to make the comparison easier, the calculated spectrum has been convoluted by a 50 $cm^{-1}$ FWHM Lorentzian profile (dotted line in Fig. 3).

Overall a good match is obtained between the experimental and the theoretical spectra. It should be noted that a scaling factor of 0.98 has been applied to the calculated frequencies. This scaling factor has been derived by comparing B3LYP with experimental infrared spectrum [21] in the case of the free but-1-ene ligand. This is, in particular, the case for the three most intense transitions: the C=C stretch is predicted at 1697 $cm^{-1}$ (versus 1642 $cm^{-1}$ experimentally), the wagging of the ethylenic *CH2at*938 cm-1 (914 $cm^{-1}$), and the twisting of the ethylenic $CH_2$ at 1010 $cm^{-1}$ (994 $cm^{-1}$). Considering this redshift effect, one can interpret the experimental spectrum of ${FeC_4H_8}^+$ as follows. At long wavelengths, the two main transitions observed can be assigned to the two main predicted infrared harmonic transitions. The observed maximum absorption at 950 $cm^{-1}$ should correspond to the out-of-plane ethylenic $CH_2$ wagging predicted at 972 $cm^{-1}$, whereas the second maximum at 1035 $cm^{-1}$ should be assigned to the $CH_2$ twist (1071 $cm^{-1}$). At higher energies, the broad band with a maximum absorption at 1459 $cm^{-1}$ should be the result of the convolution of five relatively intense calculated transitions. Considering the redshift at lower energy, it seems reasonable to attribute the maximum absorption found at 1459 $cm^{-1}$ to three modes predicted as intense by theory: angular deformation of the ethyl-$CH_2$ (1483) and $CH_3$ (1489 and 1500 $cm^{-1}$) groups. The broadening of the band is also due to the fact that, slightly higher in energy (1530 $cm^{-1}$), one finds the normal mode corresponding to the C=C stretch which is predicted as the most intense. A relatively intense absorption is also predicted slightly lower in energy (1448 $cm^{-1}$), the normal mode essentially corresponding to an in-plane *d* (ethylenic-$CH_2$) deformation.

The good match between experiment and theory strongly suggests that no rearrangement occurs during the generation of the ${FeC_4H_8}^+$ ions, and that the process is a simple displacement of CO from mass-selected $Fe(CO)^+$ by but-1-ene. It is interesting to note that, over the wavelengths studied, the relative predicted IR intensities parallel the one derived from the IRMPD. This is consistent with the dependence of the fragmentation efficiency of ${Fe(CO)_5}^+$ on the laser intensity described above.

This first example of coupling an FT-ICR-MS with IR-FEL opens the way to direct structural characterization of the variety of ions that can be selectively prepared in an FT-ICR-MS. Infrared spectroscopy of reactive intermediates can be derived, thus offering an interesting alternative to matrix isolation technique [22] for which the species cannot always be clearly assigned. Whereas only the primary ions of PAH have been studied [11], the FT-ICR-MS will allow for the preparation of PAH ions with a controlled C/H ratio, which are potentially of astrophysical interest. The present experimental setup should also highly contribute to the ongoing effort of the mass spectrometry community towards the understanding of the interactions of biological molecules in the gas phase.

We are grateful to R. Herren and J.-R. Bazouin for their contribution to the conception of MICRA. We also thank R. Prazeres and G. Humbert at CLIO for their uncompromising support.

---

*Corresponding author.
Email address: philippe.maitre@lcp.u-psud.fr

[1] *Organometallic Ion Chemistry*, edited by B. S. Freiser (Kluwer, Dordrecht, 1996).

[2] A. G. Marshall, Int. J. Mass Spectrom. **200**, 331 (2000).

[3] K. Ervin, Chem. Rev. **101**, 391 (2001).

[4] R. J. Saykally, Science **239**, 157 (1988).

[5] T. Oka, Phys. Rev. Lett. **45**, 531 (1980).

[6] G. Gregoire and M. A. Duncan, Chem. Phys. Lett. **349**, 77 (2001).

[7] M. Okumura, L. Yeh, and Y. Lee, J. Chem. Phys. **83**, 3705 (1985).

[8] R. Prazeres, F. Glotin, C. Insa, D. Jaroszynski, and J. M. Ortega, Eur. Phys. J. D **3**, 87 (1998).

[9] J. Oomens, A. J. A. van Roij, G. Meijer, and G. von Helden, Astrophys. J. **542**, 404 (2000).

[10] J. Oomens, G. Meijer, and G. von Helden, J. Phys. Chem. A **105**, 8302 (2001).

[11] J. Oomens, B. G. Sartakov, A. Tielens, G. Meijer, and G. von Helden, Astrophys. J. **560**, L99 (2001).

[12] D. van Heijnsbergen, G. von Helden, G. Meijer, P. Maitre, and M. Duncan, J. Am. Chem. Soc. **124**, 1562 (2002).

[13] R. L. Woodin, D. S. Bomse, and J. L. Beauchamp, J. Am. Chem. Soc. **100**, 3248 (1978).

[14] J. Black, E. Yablonovitch, N. Bloembergen, and S. Mukamel, Phys. Rev. Lett. **38**, 1131 (1977).

[15] G. Dietrich, S. Krückeberg, K. Lützenkirchen, L. Schweikhard, and C. Walther, J. Chem. Phys. **112**, 752 (2000).

[16] S. Le Caër, M. Heninger, P. Pernot, and H. Mestdagh, Phys. Chem. Chem. Phys. **4**, 1855 (2002).

[17] A. Simon, L. MacAleese, P. Boissel, and P. Maitre, Int. J. Mass Spectrom. **219**, 457 (2002).

[18] P. I. Surya, L. M. Roth, D. R. A. Ranatunga, and B. S. Freiser, J. Am. Chem. Soc. **118**, 1118 (1996).

[19] M. Frisch *et al.*, GAUSSIAN 98 PROGRAM, Gaussian Inc., Pittsburgh, PA, 1998.

[20] M. Sodupe, C.W. Bauschlicher, Jr., S. R. Langhoff, and H. Partridge, J. Phys. Chem. **96**, 2118 (1992).

[21] *NIST Chemistry WebBook, NIST Standard Reference Database Number 69*, edited by P. Linstrom and W. Mallard (National Institute of Standards and Technology, Gaithersburg, MD, 2001).

[22] M. Zhou, L. Andrews, and W. J. Bauschlicher, Chem. Rev. **101**, 1931 (2001).